

## Cadherin and Integrin Regulation of Epithelial Cell Migration

Jonathan Silvestre

*Department of Chemical & Biomolecular Engineering, University of Illinois at Urbana–Champaign, Urbana, Illinois 61801*

Paul J. A. Kenis

*Department of Chemical & Biomolecular Engineering, Institute for Genomic Biology, University of Illinois at Urbana–Champaign, Urbana, Illinois 61801*

Deborah E. Leckband\*

*Department of Chemical & Biomolecular Engineering, Institute for Genomic Biology, University of Illinois at Urbana–Champaign, Urbana, Illinois 61801**Received March 30, 2009. Revised Manuscript Received June 8, 2009*

These studies quantified the relative effects of E-cadherin expression and homophilic ligation on the integrin-mediated motility of epithelial cells. Micropatterned proteins were used to quantitatively titrate the ligation of E-cadherin and integrin receptors in order to assess their coordinate influence on the migration velocities of MDA-MB-231 breast tumor epithelial cells. Fibronectin, E-cadherin, and mixtures of fibronectin and E-cadherin were covalently patterned on solid surfaces at defined compositions and mass coverages. The migration velocities of parental epithelial cells and of cells engineered to express E-cadherin under tetracycline control show that E-cadherin expression reduces cell motility by both adhesion-dependent and adhesion-independent mechanisms. Increasing E-cadherin expression levels also suppresses the dependence of cell velocity on the fibronectin coverage. On E-cadherin-containing substrata, the cell velocity decreases both with the E-cadherin expression level and with the immobilized E-cadherin surface density. These studies thus identified conditions under which E-cadherin preferentially suppresses cell migration by adhesion-independent versus adhesion-dependent mechanisms.

## Introduction

Cancer metastasis involves the disruption of cell–cell contacts, cell escape from tumors, and reattachment at distal sites in the body. In normal tissues, epithelial cells strongly adhere via cadherins, which are calcium-dependent cell–cell adhesion proteins. The destabilization of intercellular junctions, in either normal tissue remodeling or in the progression of diseases such as cancer, involves the disruption of cadherin junctions by mechanisms that include proteolytic shedding, internalization, or the altered expression of epithelial cadherin (E-cadherin).<sup>1–3</sup> In metastasis, such changes facilitate cell detachment from the primary tumor site.<sup>4,5</sup>

E-cadherin is a tumor suppressor that inhibits both cell proliferation and invasiveness.<sup>6</sup> The loss or decrease in E-cadherin expression and/or function in cancer cells typically correlates with

high invasiveness and metastasis.<sup>5,7–12</sup> Increased invasive behavior requires the loss of intercellular adhesion, which could arise from intracellular signaling, loss of adhesive strength, and/or aberrant interactions with the extracellular matrix (ECM). Several studies suggest that E-cadherin impedes cell migration and invasiveness by homophilic E-cadherin adhesion.<sup>9,13–15</sup> At low cell densities, mouse fibroblasts transfected with E-cadherin migrated through gels, but confluent cell densities inhibited the migration.<sup>14</sup> The addition of anti-E-cadherin antibodies, which blocked cadherin-dependent adhesion, restored cell migratory behavior. Transfecting fibroblasts with E-cadherin similarly suppressed cell infiltration of collagen gels in an E-cadherin-dependent manner.<sup>9</sup>

Other studies indicate that E-cadherin expression alters cell migration by an adhesion-independent mechanism. The expression of E-cadherin regulates levels of cytosolic  $\beta$ -catenin.<sup>6,16,17</sup> Wong and Gumbiner reported that  $\beta$ -catenin binding to the cytodomain of E-cadherin attenuated cell motility in an adhesion-independent manner.<sup>17</sup> The cytodomain of E-cadherin binds

\*Corresponding author. E-mail: Leckband@illinois.edu.

(1) Chappuis-Flament, S.; Wong, E.; Hicks, L. D.; Kay, C. M.; Gumbiner, B. M. *J. Cell Biol.* **2001**, *154*(1), 231–243.

(2) Cavallaro, U.; Christofori, G. *Nat. Rev. Cancer* **2004**, *4*(2), 118.

(3) Janda, E.; Nevolo, M.; Lehmann, K.; Downward, J.; Beug, H.; Grieco, M. *Oncogene* **2006**, *25*(54), 7117–7130.

(4) Hazan, R. B.; Qiao, R.; Keren, R.; Badano, I.; Suyama, K. *Ann. N.Y. Acad. Sci.* **2004**, *1014*, 155–163.

(5) Takeichi, M. *Curr. Opin. Cell Biol.* **1993**, *5*(5), 806–811.

(6) Christofori, G.; Semb, H. *Trends Biochem. Sci.* **1999**, *24*(2), 73–76.

(7) Berx, G.; Cleton-Jansen, A. M.; Nollet, F.; de Leeuw, W. J.; van de Vijver, M.; Cornelisse, C.; van Roy, F. *EMBO J.* **1995**, *14*(24), 6107–15.

(8) Cowin, P.; Rowlands, T. M.; Hatsell, S. J. *Curr. Opin. Cell Biol.* **2005**, *17*(5), 499–508.

(9) Frixen, U. H.; Behrens, J.; Sachs, M.; Eberle, G.; Voss, B.; Warda, A.; Lochner, D.; Birchmeier, W. *J. Cell Biol.* **1991**, *113*(1), 173–185.

(10) Qureshi, H. S.; Linden, M. D.; Divine, G.; Raju, U. B. *Am. J. Clin. Pathol.* **2006**, *125*(3), 377–385.

(11) Sommers, C. L.; Byers, S. W.; Thompson, E. W.; Torri, J. A.; Gelmann, E. P. *Breast Cancer Res. Treat* **1994**, *31*(2–3), 325–335.

(12) Sommers, C. L.; Thompson, E. W.; Torri, J. A.; Kemler, R.; Gelmann, E. P.; Byers, S. W. *Cell Growth Differ.* **1991**, *2*(8), 365–372.

(13) Behrens, J.; Mareel, M. M.; Van Roy, F. M.; Birchmeier, W. *J. Cell Biol.* **1989**, *108*(6), 2435–2447.

(14) Chen, W. C.; Obrink, B. *J. Cell Biol.* **1991**, *114*(2), 319–327.

(15) Vlemminckx, K.; Vakaet, L. Jr.; Mareel, M.; Fiers, W.; van Roy, F. *Cell* **1991**, *66*(1), 107–119.

(16) Gottardi, C. J.; Wong, E.; Gumbiner, B. M. *J. Cell Biol.* **2001**, *153*(5), 1049–1060.

(17) Wong, A. S.; Gumbiner, B. M. *J. Cell Biol.* **2003**, *161*(6), 1191–1203.

p120 catenin (p120<sup>ctn</sup>), and recent findings suggest that a p120<sup>ctn</sup>-dependent pathway may impede motility.<sup>18,19</sup>

The coordinated interplay between cadherins and integrins also regulates the structural integrity of tissues. In vivo, cell emigration from tumors or cell migration into wound sites also results from the disruption of intercellular contacts and promotion integrin-mediated cell migration. In myoblasts, cadherins and integrins coordinate migration cessation by contact inhibition, which results from synergistic signaling between the  $\alpha 5$  integrin and neural-cadherin.<sup>20</sup> Conversely, integrin activation can destabilize cell–cell junctions. The mechanical stimulation of integrins in vascular endothelial cells disrupted cell–cell junctions.<sup>21</sup> Integrin signaling and elevated Src activity similarly deregulate E-cadherin in colon carcinoma cells and are associated with the epithelial-to-mesenchymal transition.<sup>22,23</sup>

In many of these examples, it is unclear whether enhanced cell motility is due to reduced E-cadherin adhesion or whether E-cadherin down regulation alone confers a motile phenotype. In the context of metastasis, determining the principal mechanism(s) of migration suppression by E-cadherin is central to establishing the molecular basis of disease as well as for identifying therapies for preventing disease progression. The ability to interrogate mechanisms by which E-cadherin and integrins coordinately regulate cell migration is currently limited, in part, by the methods used to investigate cell motility.

Many platforms commonly used to study cell migration and invasion are end-point assays that do not directly observe cells or control the cell environment. For example, studies of cell migration and invasion often use wound healing assays or filter-based platforms such as Boyden chambers. Wound healing assays inherently include (uncontrolled) cell–cell interactions, cell migration, and cell proliferation.<sup>24,25</sup> Cell proliferation and migration into the wound are not uniform during the experiment, and they depend on the proximity of cells to the wound.<sup>25</sup> Boyden chambers and similar filter-based assays determine cell migration rates from the redistribution of a cell population as cells migrate through a filter.<sup>26</sup> This end-point analysis does not allow direct observations of cell movement. Quantitative determinations of cell velocity, directionality, and persistence therefore require model fits to empirical data.<sup>27</sup> These assays also use large numbers of cells, but only a small percentage of them migrate. This renders the data difficult to interpret.<sup>24</sup>

Additional substrata consist of uncoated filters or filters coated with Matrigel, collagen, fibrin, and other matrix proteins.<sup>9,13,14,17,28–30</sup> These materials contain ligands for integrins

but not cadherins. Furthermore, the ligand surface density is not easily amendable. Alternatively, surface chemical approaches, which afford better control of the ligand identity and surface coverage on two-dimensional substrata, have been used extensively to investigate adhesion-dependent cell behavior.<sup>27,31–38</sup> These platforms also enable the direct visualization of individual cells as they migrate over ligand fields and were used to demonstrate the dependence of integrin-mediated cell migration on ligand density.<sup>31–33</sup> Surface chemical approaches also enabled quantitative investigations of the synergistic effects of two different adhesion receptors on cell rolling.<sup>35,36</sup>

This study used immobilized protein patterns to investigate cross-talk between cadherins and integrins in the regulation of cell migration. Specifically, we used defined, fabricated patterns of integrin and E-cadherin ligands to quantify the impact of E-cadherin expression and homophilic ligation on epithelial cell migration. These studies also used the highly motile, metastatic MDA-MB-231 human breast cancer cell line (231 cells). A second MDA-MB-231 cell line engineered to express E-cadherin under tetracycline control (231-Tet cells) enabled the manipulation of E-cadherin expression levels. Protein patterning and automated cell tracking enabled rapid titrations of the influence of E-cadherin expression and ligation on cell movement on a variety of quantitatively defined substrata consisting of fibronectin, E-cadherin, or fibronectin/E-cadherin mixtures. These findings confirm that E-cadherin expression alone substantially attenuates cell motility. They also demonstrate conditions under which homophilic E-cadherin ligation is the predominant mechanism suppressing cell migration.

## Materials and Methods

**Reagents.** The Fc-tagged canine E-cadherin ectodomain was purified as described by Chappuis-Flament et al.<sup>1</sup> Fibronectin from bovine plasma and bovine serum albumin (BSA) were from Sigma Aldrich. 16-Mercaptohexadecanoic acid (MHD) [purity > 98.5%] and 11-mercaptoundecan-1-ol (MUD) [purity > 98%] were purchased from Aldrich Chemical Co. The linkers 1-ethyl-3-(3-dimethylaminopropyl) carbodiimide HCl (EDC) and *N*-hydroxysuccinimide (NHS) were from Pierce. Borosilicate glass substrata were from Fisher Scientific.

**Cell Culture.** MDA-MB-231 human breast tumor cells, purchased from ATCC, and MDA-MB-231Tet cells (a gift from Dr. Gottardi, Northwestern, IL) were cultured in Leibovitz's L-15 medium supplemented with 10% fetal bovine serum (FBS, Hyclone) and penicillin–streptomycin (HyQ). Cells were maintained at 37 °C in a humidified incubator. Transfected cells were selected as described by Wong and Gumbiner.<sup>17</sup> Briefly, 400  $\mu\text{g}/\text{mL}$  of G418 (Calbiochem) and 800  $\mu\text{g}/\text{mL}$  of hygromycin b (Invitrogen) were added to the subculture after each passage. Cell monolayers were dissociated by incubation with 0.01% (w/v) trypsin (Gibco) with 2 mM  $\text{Ca}^{2+}$  for 5 min at 37 °C. It is well established that cadherin is not degraded by trypsin in 2 mM calcium. Similarly,

(18) Yanagisawa, M.; Anastasiadis, P. Z. *J. Cell Biol.* **2006**, *174*(7), 1087–1096.

(19) Yanagisawa, M.; Huveldt, D.; Kreinest, P.; Lohse, C. M.; Chevillat, J. C.; Parker, A. S.; Copland, J. A.; Anastasiadis, P. Z. *J. Biol. Chem.* **2008**, *283*(26), 18344–18354.

(20) Huttenlocher, A.; Lakonishok, M.; Kinder, M.; Wu, S.; Truong, T.; Knudsen, K. A.; Horwitz, A. F. *J. Cell Biol.* **1998**, *141*(2), 515–526.

(21) Wang, Y.; Jin, G.; Miao, H.; Li, J. Y.; Usami, S.; Chien, S. *Proc. Natl. Acad. Sci. U.S.A.* **2006**, *103*(6), 1774–1779.

(22) Avizienyte, E.; Wyke, A. W.; Jones, R. J.; McLean, G. W.; Westhoff, M. A.; Brunton, V. G.; Frame, M. C. *Nat. Cell Biol.* **2002**, *4*(8), 632–638.

(23) Avizienyte, E.; Frame, M. C. *Curr. Opin. Cell Biol.* **2005**, *17*(5), 542–547.

(24) Entschladen, F.; Drell, T. L. t.; Lang, K.; Masur, K.; Palm, D.; Bastian, P.; Niggemann, B.; Zaenker, K. S. *Exp. Cell Res.* **2005**, *307*(2), 418–426.

(25) Zahm, J. M.; Kaplan, H.; Herard, A. L.; Doriot, F.; Pierrot, D.; Somelette, P.; Puchelle, E. *Cell Motil Cytoskeleton* **1997**, *37*(1), 33–43.

(26) Boyden, S. J. *Exp. Med.* **1962**, *115*, 453–466.

(27) Buettner, H. M.; Lauffenburger, D. A.; Zigmond, S. H. *J. Immunol. Methods* **1989**, *123*(1), 25–37.

(28) Islam, L. N.; McKay, I. C.; Wilkinson, P. C. *J. Immunol. Methods* **1985**, *85*(1), 137–151.

(29) Fong, C. J.; Sutkowski, D. M.; Kozlowski, J. M.; Lee, C. *Invasion Metastasis* **1992**, *12*(5–6), 264–274.

(30) Bartsch, J. E.; Staren, E. D.; Appert, H. E. *J. Surg. Res.* **2003**, *110*(1), 287–294.

(31) Palecek, S. P.; Loftus, J. C.; Ginsberg, M. H.; Lauffenburger, D. A.; Horwitz, A. F. *Nature* **1997**, *385*(6616), 537–540.

(32) DiMilla, P. A.; Stone, J. A.; Quinn, J. A.; Albelda, S. M.; Lauffenburger, D. A. *J. Cell Biol.* **1993**, *122*(3), 729–737.

(33) Palecek, S. P.; Schmidt, C. E.; Lauffenburger, D. A.; Horwitz, A. F. *J. Cell Sci.* **1996**, *109*(5), 941–952.

(34) Lauffenburger, D. A. *Annu. Rev. Biophys. Biophys. Chem.* **1991**, *20*, 387–414.

(35) Eniola, A. O.; Willcox, P. J.; Hammer, D. A. *Biophys. J.* **2003**, *85*(4), 2720–2731.

(36) Bhatia, S. K.; King, M. R.; Hammer, D. A. *Biophys. J.* **2003**, *84*(4), 2671–2690.

(37) Yousaf, M. N.; Houseman, B. T.; Mrksich, M. *Angew. Chem., Int. Ed.* **2001**, *40*(6), 1093–1096.

(38) Mrksich, M. *Curr. Opin. Chem. Biol.* **2002**, *6*(6), 794–797.

integrins are not degraded by this mild trypsinization.<sup>39,40</sup> The cells were resuspended in 10 mL of supplemented L-15 medium and pelleted by centrifugation for 5 min at 1000 rpm using an IEC Centra 4B centrifuge equipped with a 215 rotor (IEC). Cell pellets were resuspended in serum-free L-15 medium with 2 mM Ca<sup>2+</sup>, and the cell density was determined with a hemocytometer. Cells were seeded at a density of  $2 \times 10^4$  cells/mL in the migration assays.

**Western Blots.** For Western blot analyses, cells were grown to confluence, harvested using a cell scraper, and lysed with 1% NP-40 lysis buffer (1% NP-40, 10 mM HEPES, 150 mM NaCl, 1.5 mM EDTA, pH 7.4) supplemented with protease inhibitors, as described.<sup>41</sup> Samples containing equal amounts of total protein, as determined with a colorimetric protein assay, were separated by SDS-PAGE. They were then transferred to nitrocellulose with a Trans-Blot-Semidry-Electrophoresis transfer cell (BioRad) for 30 min at 13 V. The transfer paper was incubated overnight at 4 °C with the primary mouse monoclonal antihuman E-cadherin antibody (36 clone, BD Biosciences), washed with PBS with 0.2% (v/v) Tween 20 (HyClone, Sigma), and then incubated with goat antimouse peroxidase conjugate for 1 h at room temperature. After antibody treatment, the bands were visualized with the ECL Western Blot detection kit (Pierce). After the autoradiography film (Denville Scientific) was developed (Futura 2000K, Fischer Scientific), the bands were analyzed with a Quantity One 4.6.3 densitometer (Bio-Rad). The E-cadherin expression was normalized to the total actin in the lysate. To compare expression levels in the different cells, the expression levels were also normalized against the E-cadherin expression in 231-Tet cells induced with 100  $\mu$ g/mL doxycycline.

**Flow Cytometry.** Flow cytometry was performed on a BD FACSCanto (BD Biosciences). Cells were harvested from tissue culture flasks using 0.01% (w/v) trypsin with 2 mM Ca<sup>2+</sup>, washed with Leibovitz's L-15 medium supplemented with 10% fetal bovine serum, and resuspended in phosphate buffered saline (PBS). Cells were incubated with goat polyclonal antibody directed against the extracellular domain of E-cadherin (k-20 clone, Santa Cruz Biotechnology) for 30 min at 4 °C at a concentration of 3  $\mu$ g/mL. Unbound primary antibodies were removed by washing three times with PBS. The cells were then resuspended in PBS containing 2 mM calcium and incubated in the dark with 3  $\mu$ g/mL PE-Cy5-conjugated mouse anti-goat IgG (Santa Cruz Biotechnology) for 30 min at 4 °C. Cells were analyzed using FACS Express 3.0 (De Novo). As a negative control, cells were incubated with secondary antibody only. E-cadherin surface densities were quantified from the amount of bound PE-Cy5 antibody. The fluorescence was calibrated with Quantum PE-Cy5 MESF fluorescent calibration microspheres (Bangs Laboratories, Inc.). A standard calibration curve was used to convert the fluorescence intensity to protein surface coverage on the cells.

**Preparation of Uniform Protein Patterns with Microfluidic Devices.** The protein was covalently immobilized on self-assembled monolayers (SAMs) of carboxylic acid-terminated alkanethiols. SAMs were assembled on thermally evaporated gold films deposited on glass microscope slides, as described previously.<sup>42,43</sup> The gold-coated slides were immediately immersed in an ethanolic solution of 3:1 molar ratio of mercapto hexadecanoic acid:mercaptoundecanol for 24 h, rinsed with ethanol, and dried with filtered N<sub>2</sub>. A PDMS mold containing the microfluidic network was then brought into conformal contact

with the slide. The microchannels were then flushed with ethanol, followed by PBS containing 2 mM Ca<sup>2+</sup>. The carboxylic acid terminated alkanethiols were activated with EDC/NHS at concentrations of 3.8 and 7.6 mg/mL, respectively. Protein solutions were then injected through the microchannels at a flow rate of 0.1 mL/h, with a total volume of 0.2 mL infused. Following the protein injection, the microchannels were rinsed with 0.2 mL of PBS buffer with Ca<sup>2+</sup>. After removing the PDMS mold, the chip was immersed in 10% (w/v) BSA in PBS for 30 min, to prevent nonspecific cell adhesion.

**Cell Migration on Patterned Substrata.** Cells were seeded on uniform, protein-coated substrata in a 35 mm Petri dish (BD Falcon) at a density of  $2 \times 10^4$  cells/mL in serum-free L-15 medium supplemented with 2 mM Ca<sup>2+</sup>. The cell medium was then covered with 5 mL of sterile mineral oil (Sigma) to minimize heat loss and water evaporation during the measurements. The Petri dish was placed on a machined metal holder used to maintain the temperature at 37 °C by circulating water through the metal holder. The holder was fastened to the stage of an inverted Zeiss Axiovert 200 microscope equipped with a 10 $\times$  objective. Cells were allowed to attach to the substrata for 3 h before tracking cell movement. The cell movements on the substrata were monitored with an AxioCam high performance monochrome digital camera and recorded every 15 min for 12 h, using Axiovision software version 4.6.

A high resolution, a programmable scanning stage enabled us to track multiple cells in at least three regions per substratum composition investigated. Regions near the edges of the patterns were avoided to minimize contributions from anomalous migration at boundaries. Duplicate experiments were conducted for all experimental conditions. For each set of conditions, 20–40 individual cells were tracked. Cell locations were defined by the cell centroid and were manually tracked using the Manual Tracking plugin for ImageJ (Fabrice Cordelieres, Institut Curie, NIH). Cell position and distance traveled were recorded frame-to-frame. The effective cell velocity was calculated according to:<sup>44</sup>  $V_{\text{eff}} = S/t$ , where  $S$  is the total cell migration path length and  $t$  is the recording time. Taking into account intervals where the cell did not move, the real velocity is  $V_{\text{real}} = S/(t - N)$ , where  $N$  is the number of time intervals during which the cell did not move, expressed in minutes.<sup>44</sup> Data are presented as the mean  $\pm$  SD. The Unpaired Student's  $t$ -test was used to determine the statistical significance of differences between individual measurements, and differences between groups were determined with the ANOVA (Excel, Microsoft).  $P$  values  $< 0.05$  were considered to be statistically significant.

**Surface Plasmon Resonance (SPR) Measurements.** The surface densities of fibronectin and E-cadherin covalently bound to SAMs were determined with a home-built surface plasmon resonance (SPR) instrument.<sup>45</sup> The SPR flow cell containing the SAM-modified gold substrate was initially rinsed with water and PBS buffer with Ca<sup>2+</sup> for 15 min. The carboxylic acid terminated alkanethiols were then activated with EDC/NHS coupling agents<sup>42</sup> for 15 min at a flow rate of 4 mL/h, followed by rinsing with PBS buffer with Ca<sup>2+</sup> for 5 min. The protein was then introduced at a flow rate of 0.1 mL/h. After the adsorbed amount stabilized, the SPR cell was rinsed with PBS buffer with Ca<sup>2+</sup> for 10 min at a flow rate of 4 mL/min. The surface density of the bound protein was determined by fitting the Fresnel reflectivity equations to the change in the plasmon resonance angle following the protein adsorption.

The measured plasmon resonance angle was recorded over the time-course of the experiment. The shift in the resonance angle was then determined from  $\Delta\theta = \theta_t - \theta_{t_0}$  where  $\theta_{t_0}$  is the initial plasmon resonance angle prior to protein binding and  $\theta_t$  is the final plasmon resonance angle after protein deposition.

(39) Brown, M. A.; Wallace, C. S.; Anamelechi, C. C.; Clermont, E.; Reichert, W. M.; Truskey, G. A. *Biomaterials* **2007**, *28*(27), 3928–3935.

(40) Wong, N. C.; Mueller, B. M.; Barbas, C. F.; Ruminski, P.; Quaranta, V.; Lin, E. C.; Smith, J. W. *Clin. Exp. Metastasis* **1998**, *16*(1), 50–61.

(41) Yap, A. S.; Niessen, C. M.; Gumbiner, B. M. *J. Cell Biol.* **1998**, *141*(3), 779–789.

(42) Gunawan, R. C.; Chohan, E. R.; Conour, J. E.; Silvestre, J.; Schook, L. B.; Gaskins, H. R.; Leckband, D. E.; Kenis, P. J. *Langmuir* **2005**, *21*(7), 3061–3068.

(43) Gunawan, R. C.; Silvestre, J.; Gaskins, H. R.; Kenis, P. J.; Leckband, D. E. *Langmuir* **2006**, *22*(9), 4250–4258.

(44) Wojciak-Stothard, B.; Denyer, M.; Mishra, M.; Brown, R. A. *In Vitro Cell. Dev. Biol.: Anim.* **1997**, *33*(2), 110–117.

(45) Lavrik, N.; Leckband, D. *Langmuir* **2000**, *16*, 1842–1851.

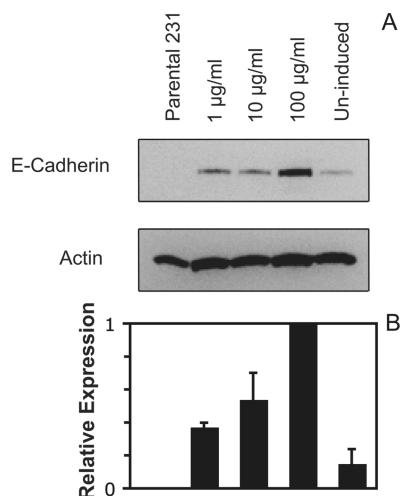


**Figure 1.** (A) Western blots of equivalent micrograms of lysates from parental 231 cells and 231-Tet cells treated with different concentrations of doxycycline. The lysates were analyzed using a mouse antihuman E-cadherin mAb (BD Bioscience). The total actin was used as an internal standard. (B) Plot of the E-cadherin expression levels in the different cells in (A) relative to the E-cadherin expressed in cells treated with 100 µg/mL doxycycline. The E-cadherin expression in the different cells was normalized to total actin in the lysate.

A theoretical angle was determined with the IGOR-based (Wavemetrics) four-phase Fresnel reflectivity equation (Corn laboratory, UC Irvine). The change in angle recorded by SPR was added to the theoretical angle, and the effective refractive index of the protein layer ( $n_{\text{eff}}$ ) was calculated using a five-phase Fresnel reflectivity equation (Corn laboratory, UC Irvine). The volume fraction of the protein ( $x_p$ ) was calculated from  $\chi_p = (n_{\text{eff}} - n_{\text{H}_2\text{O}})/(n_p - n_{\text{H}_2\text{O}})$  where  $n_p$  and  $n_{\text{H}_2\text{O}}$  are the refractive indices of protein and water, respectively. We used a refractive index of 1.46 for fibronectin and E-cadherin.<sup>46</sup> The protein coverage was determined from the volume fraction as described previously.<sup>42</sup>

## Results

**E-Cadherin Expression in Epithelial Cells.** The relative expression levels of E-cadherin in the parental 231 and engineered 231-Tet cells were first assessed by Western blot analysis. Western blots (Figure 1A) confirmed that parental 231 cells do not express E-cadherin, in agreement with published data.<sup>47</sup> The uninduced 231-Tet cells do exhibit some E-cadherin expression, indicating that this inducible expression system is somewhat “leaky”. However, the densitometry scans of the immunoblots do show that doxycycline treatment 24 h prior to the assays increases the E-cadherin expression in a doxycycline-concentration-dependent manner. The relative E-cadherin expression was normalized to total actin in the cell lysate. Figure 1B shows the relative increase in E-cadherin expression with doxycycline concentration.

FACS measurements then estimated the E-cadherin expression levels on the MDA-MB-231 (231) and on the tetracycline inducible MDA-MB-231 (231-Tet) cells. Induced 231-Tet cells were cultured in the presence of doxycycline for 24 h prior to flow cytometry assays. The E-cadherin surface densities, estimated by FACS and the use of Quantum PE-Cy5 MESF fluorescent calibration beads, were  $20 \pm 1$  and  $46 \pm 2$  molecules/ $\mu\text{m}^2$  for cells treated with 1 and 100 µg/mL doxycycline, respectively. The

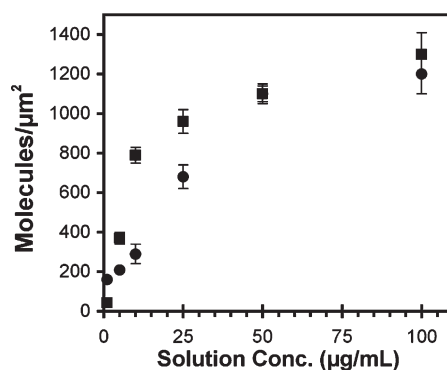


**Figure 2.** Surface densities of E-cadherin (circles) and fibronectin (squares) as a function of the bulk protein concentration. The protein was covalently bound to carboxy-terminated alkanethiol monolayers, as described in the text. The immobilized protein density (molecules/ $\mu\text{m}^2$ ) was determined as a function of the bulk protein concentration (µg/mL) by SPR.

uninduced 231-Tet cells expressed  $18 \pm 1$  cadherins/ $\mu\text{m}^2$ , based on these FACS measurements.

**Protein Surface Densities on Patterned Substrata.** Microfluidic platforms were used to generate protein patterns with defined composition and mass coverage. These substrata allow the direct visualization of cells, and therefore the use of time-lapse microscopy for direct measurements of random cell motility. This patterning also enables assessments of the effect of the protein density and composition on cell migration velocities.

The amount of bound protein was determined from a surface plasmon resonance calibration curve obtained by determining the amount of adsorbed cadherin or fibronectin at a given bulk concentration and adsorption time. The adsorbed protein densities obtained at each bulk protein concentration were plotted against the solution concentration to generate an “adsorption isotherm” such as in Figure 2. The adsorbed amount was also validated with isotopically labeled protein.

**Cell Migration on “One-Component” Uniform Substrata.** *Fibronectin Substrata (BSA Backfill).* To determine the relative effect of E-cadherin expression on integrin-dependent cell migration on the extracellular matrix protein fibronectin, we quantified the random migration velocities of 231 and 231-Tet cells on fibronectin substrata. Fibronectin engages the  $\alpha_v\beta_1$  and  $\alpha_3\beta_1$  integrins expressed by 231 cells.<sup>30,40,48</sup> Bartsch et al. reported that as little as 1 µg/mL of physisorbed fibronectin promoted the adhesion and migration of MDA-MB-231 and MDA-MB-435 cells.<sup>30</sup> However, physisorbed fibronectin can desorb over the course of the measurement. These studies instead used covalently bound fibronectin to provide a more robust substratum for cell migration studies. Any differences between the migratory behavior of parental 231 cells and the transformed 231 cells could therefore be attributed to E-cadherin expression.

Wind-rose plots indicate that cells on these substrata exhibited random, persistent walks. The standard observation time was 12 h, but the cell migration velocities were statistically similar for 8 and 16 h observation times. The migration velocities of the parental 231 cells exhibited the biphasic dependence on the fibronectin surface density that is typical of migrating cells on the extracellular matrix (Figure 3A).<sup>31</sup> At the fibronectin surface densities of 960 and 1100 molecules/ $\mu\text{m}^2$ , the migration velocities were highest at  $29 \pm 5$  and  $28 \pm 5$   $\mu\text{m}/\text{h}$  (Figure 3A). A Student’s *t*-test (Excel, Microsoft) showed that the highest migration

(46) Guemouri, L.; Ogier, J.; Ramsden, J. *J. Chem. Phys.* **1998**, *109*, 3265–3268.

(47) Pierceall, W. E.; Woodard, A. S.; Morrow, J. S.; Rimm, D.; Fearon, E. R. *Oncogene* **1995**, *11*(7), 1319–1326.

(48) Lichtner, R. B.; Howlett, A. R.; Lerch, M.; Xuan, J. A.; Brink, J.; Langton-Webster, B.; Schneider, M. R. *Exp. Cell Res.* **1998**, *240*(2), 368–376.

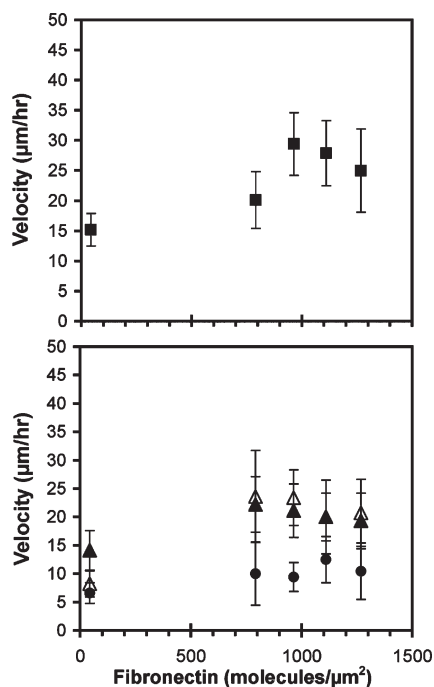


**Figure 3.** Cell migration velocity on fibronectin substrata (BSA backfill). (A) The velocity of parental 231 cells (filled squares) was determined as a function of the fibronectin density. (B) The velocity of 231-Tet cells induced with 1  $\mu\text{g}/\text{mL}$  and 100  $\mu\text{g}/\text{mL}$  doxycycline (filled triangles and filled circles, respectively), and uninduced 231-Tet cells (empty triangles) were determined as a function of the fibronectin density.

velocity of 29  $\mu\text{m}/\text{h}$  was statistically greater than the migration velocities observed at the lowest and highest fibronectin densities ( $p < 0.05$ ).

E-cadherin expression had two effects on random cell migration on fibronectin. First, the expression alone attenuated the cell migration velocity. Second, the migration velocities of the 231-Tet cells appeared to be independent of the fibronectin density, within experimental error. The magnitude of the change depended on the E-cadherin expression level. At low E-cadherin expression levels, the migration velocity on substrata containing  $40 \pm 8$  or  $790 \pm 40$  fibronectin/ $\mu\text{m}^2$  was indistinguishable from the parental 231 cells. A student's *t*-test confirmed that the migration velocities of the induced (1  $\mu\text{g}/\text{mL}$ ), and uninduced 231-Tet cells were statistically similar to the parental cells ( $p > 0.05$ ).

The velocities of the 231-Tet cells were statistically lower on fibronectin at  $960 \pm 50$  molecules/ $\mu\text{m}^2$  ( $p < 0.05$ ). At  $> 790$  fibronectin/ $\mu\text{m}^2$ , the cell migration rates clearly decreased with the E-cadherin expression (Figure 3B) ( $p < 0.05$ ). On films supporting the highest cell migration velocities (960 and 1100 fibronectin/ $\mu\text{m}^2$ ), the motility of the uninduced 231-Tet cells was  $\sim 20\%$  lower than the parental 231 cells ( $p < 0.05$ ). Treating 231-Tet cells with 1  $\mu\text{g}/\text{mL}$  doxycycline decreased motility by  $\sim 30\%$  ( $p < 0.05$ ). Further increasing the E-cadherin expression to  $\sim 46$  molecules/ $\mu\text{m}^2$  with 100  $\mu\text{g}/\text{mL}$  doxycycline reduced the migration velocity by  $\sim 60\%$  ( $p < 0.05$ ).

Interestingly, the E-cadherin expression alone affected the dependence of the migration velocity on the fibronectin density. The 231-Tet cells, which express low levels of E-cadherin (cf. Figure 1), exhibited a weaker dependence on the fibronectin surface density than the parental 231 cells (Figure 3B). Namely, the maximum was less pronounced and the velocities at the higher fibronectin densities were lower. With the 231-Tet cells treated

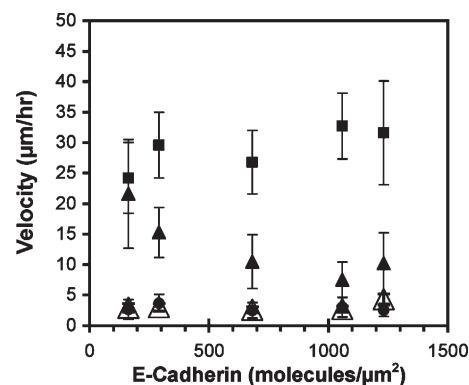


**Figure 4.** Cell migration velocities on E-cadherin substrata (BSA backfill). The velocities of parental 231 cells (filled squares) and 231-Tet cells induced with 1 and 100  $\mu\text{g}/\text{mL}$  doxycycline (filled triangles and filled circles, respectively) were determined as a function of the E-cadherin surface density. As a control, 1  $\mu\text{g}/\text{mL}$  induced 231-Tet cells were incubated with E-cadherin antibodies for 30 min prior to seeding (open triangles).

with 1 and 100  $\mu\text{g}/\text{mL}$ , the velocities were constant at  $19 \pm 1$  and  $10 \pm 2$   $\mu\text{m}/\text{h}$ , respectively, regardless of the fibronectin coverage (Figure 3B).

We do note that the transformed 231 Tet cell line is a single subclone of the original parental MDA-MB-231 cell line. Because cancer cell lines tend to be genetically unstable, differences between the uninduced 231 Tet cells and the parental cells could be due differences in addition to transfection with the E-cadherin expression vector. For this reason, we place more emphasis on differences in the behavior of tetracycline induced versus uninduced 231 Tet cells.

*E-Cadherin Substrata (BSA Backfill)*. In previous studies of the effects of E-cadherin on cell migration, the substrata did not contain the E-cadherin ligand. The cell migratory behavior was determined on filters or in Matrigel, which contains specific ligands for integrins but not for E-cadherin.<sup>9,13,14,17,28–30</sup> Therefore, E-cadherin ligation could only contribute to migration velocities through uncontrolled cell–cell contacts. To quantitatively control E-cadherin ligation, these studies used immobilized E-cadherin to titrate cadherin adhesion.

The parental 231 cells migrate on E-cadherin substrata (Figure 4). The velocity may increase slightly with E-cadherin coverage, but the migration rates appear to be relatively insensitive to the amount present ( $p < 0.05$ ). The 231-Tet cells treated with 1  $\mu\text{g}/\text{mL}$  doxycycline express E-cadherin ( $\sim 20$  molecules/ $\mu\text{m}^2$ ) and exhibit an inverse dependence on the E-cadherin surface density: the cell velocity decreased with increasing E-cadherin coverage. An ANOVA test confirmed that the means in the migration rates were statistically different. At  $160 \pm 10$  E-cadherin/ $\mu\text{m}^2$ , the migration velocities of the 231-Tet cells were statistically similar to those of parental 231 cells on similar substrata ( $p > 0.05$ ). However, at higher E-cadherin densities, the migration velocities of the 231-Tet cells decreased monotonically with E-cadherin and were statistically lower than the parental 231 cells on identical substrata ( $p < 0.05$ ). Increasing the E-cadherin expression level to  $\sim 46$  molecules/ $\mu\text{m}^2$  with 100  $\mu\text{g}/\text{mL}$  doxycycline completely halted migration.

The migration of parental MDA-MB-231 cells on E-cadherin was unexpected. To test whether this is specific to E-cadherin, we treated the substrata with a blocking anti-E-cadherin antibody. The antibodies prevented most cell attachment, and those few cells that attached did not migrate. This suggests that cell surface proteins might bind to the immobilized E-cadherin.

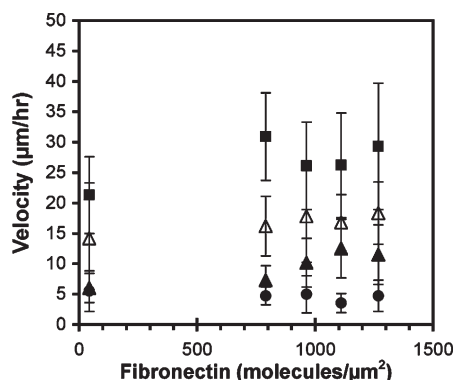


**Figure 5.** Cell velocity vs fibronectin density on mixed E-cadherin–fibronectin substrata. On these substrata, cadherin was fixed at 210 molecules/ $\mu\text{m}^2$  and the fibronectin density varied. Data are for parental 231 (filled squares) and 231Tet cells induced with 1 and 100  $\mu\text{g}/\text{mL}$  doxycycline (filled triangles and filled circles, respectively). As a control, 1  $\mu\text{g}/\text{mL}$  doxycycline induced 231Tet cells were incubated with E-cadherin antibodies for 30 min prior to seeding (open triangles).

Although MDA-MB-231 epithelial cells do not express other classical cadherins, they do express mesenchymal cadherin-11, which is not expected to bind classical E-cadherin specifically. To test for possible protein interactions that might account for the observed behavior, we used an MDA-MB-231 cell line in which cadherin-11 is stably knocked down (gift of P. Anastasiadis, Mayo Clinic, Jacksonville, FL). In contrast to the parental cells, the cadherin-11 knockdown cells did not readily attach to E-cadherin substrata and therefore did not migrate. Although this is not proof of binding between E-cadherin and cadherin-11, the inhibition of cell attachment by E-cadherin antibodies and by cadherin-11 knockdown suggests that both proteins are needed for 231 cells to migrate on E-cadherin.

**Cell Migration on Mixed Substrata.** These studies quantified the suppression of cell migration on controlled substrata containing defined amounts of both fibronectin and E-cadherin. To assess the coordinated regulation of cell movement by integrin and cadherin, mixed fibronectin–E-cadherin substrata were generated such that one protein density was fixed while the surface density of the second protein was varied. This enabled quantification of critical thresholds for “switching” from a motile to a nonmotile phenotype. We also quantified the impact of cadherin expression and adhesion on cell migration on the protein matrix.

In one set of studies, mixed substrata containing fibronectin and E-cadherin were generated such that E-cadherin was fixed at  $210 \pm 10$  molecules/ $\mu\text{m}^2$  but the fibronectin density was varied. The substrata contained E-cadherin, fibronectin, and BSA in different proportions. On these patterns, E-cadherin expression by 231-Tet cells both attenuated cell migration and altered the dependence of the migration velocity on the fibronectin density (Figure 5).

The doxycycline-treated 231-Tet cells migrated significantly slower than the parental 231 cells ( $p < 0.05$ ) on all of these mixed protein patterns. Treating 231-Tet cells with 1  $\mu\text{g}/\text{mL}$  doxycycline reduced the motility by  $\sim 60\%$  when compared to 231 cells on fibronectin substrata at the identical fibronectin density. Increasing the E-cadherin expression with 100  $\mu\text{g}/\text{mL}$  doxycycline attenuated the cell velocity by  $\sim 80\%$  on average. In the latter case, the velocities were within the noise levels.

As a control, 231-Tet cells treated with 1  $\mu\text{g}/\text{mL}$  doxycycline were preincubated with anti-E-cadherin antibodies for 30 min

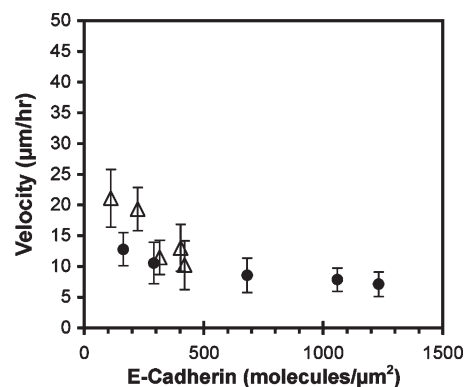


**Figure 6.** Cell velocity vs E-cadherin density on mixed E-cadherin–fibronectin substrata. In these protein films, the fibronectin was fixed at 40 molecules/ $\mu\text{m}^2$  (filled circles) and 1100 molecules/ $\mu\text{m}^2$  (open triangles) and the E-cadherin varied. The data are for 231-Tet cells treated with 1  $\mu\text{g}/\text{mL}$  doxycycline.

prior to seeding. This increased the cell migration velocity (Figure 5). The migration rates were statistically similar ( $p > 0.05$ ) to the velocities of the same cells on fibronectin substrata at the identical fibronectin densities.

The velocities of 231-Tet cells also appear to be insensitive to the fibronectin surface density. The possible exception might be the cells treated with 1  $\mu\text{g}/\text{mL}$  doxycycline ( $\sim 20$  molecules/ $\mu\text{m}^2$ ). Their velocity appears to increase with increasing fibronectin. An ANOVA test demonstrated that the 231-Tet migration rates were statistically different ( $p < 0.05$ ). However, this trend was not seen in any of the other measurements with these substrata, including those with the same cells treated with anti-E-cadherin antibodies (Figure 5).

The second series of studies used mixed fibronectin–E-cadherin substrata in which the fibronectin was fixed at  $40 \pm 8$  and  $1100 \pm 40$  molecules/ $\mu\text{m}^2$  but the E-cadherin density varied (Figure 6). The 231-Tet cells expressing  $\sim 20$  E-cadherin/ $\mu\text{m}^2$  were nearly immobile and exhibited a velocity of  $13 \pm 3$   $\mu\text{m}/\text{h}$  on 40 fibronectin/ $\mu\text{m}^2$  matrices. Increasing the E-cadherin surface density reduced the motility to  $7 \pm 2$   $\mu\text{m}/\text{h}$ .

However, when the surface density of fibronectin was maintained at 1100 molecules/ $\mu\text{m}^2$ , the decrease in the motility of 231-Tet cells treated with 1  $\mu\text{g}/\text{mL}$  doxycycline ( $\sim 20$  cadherin/ $\mu\text{m}^2$ ) with the E-cadherin surface density was more obvious. At the low cadherin densities of 110 and 220 molecules/ $\mu\text{m}^2$ , the cell velocity was highest at  $21 \pm 5$  and  $19 \pm 4$   $\mu\text{m}/\text{h}$ , respectively. At 320, 400, and 420 cadherin/ $\mu\text{m}^2$ , the cell velocity decreased to  $12 \pm 3$ ,  $13 \pm 4$ , and  $10 \pm 4$   $\mu\text{m}/\text{h}$ , respectively (Figure 6).

## Discussion and Conclusions

The microfabricated protein patterns with controlled composition described here enabled the quantitative demonstration that E-cadherin expression by MDA-MB-231 cells suppresses cell migration by both adhesion-independent and adhesion-dependent mechanisms. These findings further show that the relative contribution of either mechanism depends on the composition of the migratory substratum and on the E-cadherin expression levels.

There are apparent differences between the absolute E-cadherin surface expression determined by FACS and the relative expression levels detected by Western blot. Specifically, the FACS data suggest that the cell surface E-cadherin in uninduced 231-Tet cells and cells treated with 1  $\mu\text{g}/\text{mL}$  doxycycline are very similar despite clear differences in cell behavior (cf. Figure 4). The low

expression levels could be near the detection threshold of the antibody used or the differences may be within the standard error of these FACS measurements. Additionally, Western blots detect both cytosolic and cell surface E-cadherin. Cells could contain different amounts of cytosolic cadherin but have similar surface expression. The latter is unlikely, however, because of the clear differences in the adhesion-dependent motility reduction with induced and uninduced cells (Figure 4). The most likely explanation is that the differences between lowest expression levels are within the error of the FACS measurement. The lower expression levels are therefore considered to be semiquantitative estimates of the absolute amounts of E-cadherin on the cell surface.

The impact of changes in E-cadherin expression on epithelial cell migration on fibronectin (BSA backfill), which lacks specific E-cadherin ligands, demonstrated that E-cadherin expression alone suppresses cell motility. Cell velocity decreases with increasing E-cadherin expression. At 960–1100 fibronectin/ $\mu\text{m}^2$ , which supports the greatest motility, the velocity decreased by  $\sim 20\%$ ,  $\sim 30\%$ , and  $\sim 60\%$  at E-cadherin expression levels of roughly  $\sim 18$ ,  $\sim 20$ , and  $\sim 46$  molecules/ $\mu\text{m}^2$ .

A second observation is that E-cadherin expression altered the dependence of cell velocity on the fibronectin density. This influence is already apparent with the uninduced 231-Tet cells (Figure 3B), which express low levels of E-cadherin (cf. Figure 1). In contrast to the bell-shaped dependence of cell velocity on fibronectin density exhibited by the parental cells, the velocities of 231-Tet cells treated with 100  $\mu\text{g}/\text{mL}$  doxycycline were constant. This effect was robust and was observed on both fibronectin alone and on mixed fibronectin/E-cadherin films. The impact of E-cadherin expression on cell motility is most pronounced at fibronectin densities supporting the highest velocity of the epithelial cells.

This adhesion-independent suppression of cell motility agrees with earlier studies.  $\beta$ -catenin associates with both cell surface and cytosolic cadherin. Wong and Gumbiner used different cadherin constructs to show that E-cadherin expression alters cell motility via a  $\beta$ -catenin-dependent pathway that is independent of cadherin ligation.<sup>17</sup> Onder et al.<sup>49</sup> similarly reported that  $\beta$ -catenin regulates cell metastasis but concluded that the loss of  $\beta$ -catenin is not sufficient to promote cell invasiveness. Other recent findings suggested that E-cadherin also influences cell migration through a p120<sup>cas</sup> dependent pathway that up-regulates mesenchymal cadherin expression and inhibits RhoA.<sup>18,19</sup>

Additional studies demonstrated that E-cadherin adhesion also impedes cell motility and that this can dominate the suppression of cell migration under some conditions. Our use of controlled protein immobilization for the explicit, quantitative titration of homophilic E-cadherin adhesion demonstrated this. With the exception of the lowest immobilized E-cadherin density used, parental 231 cells migrate faster than 231-Tet cells on all E-cadherin substrata (BSA backfill). This motility may be due to a (presumably) nonspecific cadherin-11-dependent mechanism. However, E-cadherin expression switches on specific, E-cadherin-mediated adhesion and impedes the cell migration. The relative impact of the adhesion-dependent attenuation depends on both the cadherin expression level and on the immobilized E-cadherin density.

On mixed E-cadherin/fibronectin films, homophilic E-cadherin adhesion similarly impedes cell migration. Low E-cadherin expression levels ( $\sim 20/\mu\text{m}^2$ ) decreased the cell velocity by  $\sim 30\%$  on substrata containing 1100 fibronectin/ $\mu\text{m}^2$  and BSA. However,

low expression plus adhesion on films with 1100 fibronectin/ $\mu\text{m}^2$  and 460 cadherin/ $\mu\text{m}^2$  reduced cell motility by  $\sim 67\%$ . Homophilic adhesion on mixed films with high E-cadherin densities ( $> 500$  cadherin/ $\mu\text{m}^2$ ) completely blocked cell movement. Conversely, at high E-cadherin expression levels, the adhesion-independent mechanism nearly abrogates motility on fibronectin substrata but the concerted effects of high expression ( $\sim 46$  E-cadherin/ $\mu\text{m}^2$ ) and adhesive ligation completely abrogated cell movement.

That homophilic E-cadherin adhesion also suppresses motility agrees with observations that the migration of E-cadherin-expressing cells through filters depended on the cell density.<sup>14</sup> The reduced motility was attributed to homophilic cadherin ligation between contacting cells. Treatment with anti-E-cadherin antibodies, which block intercellular adhesion while maintaining cadherin expression levels, restored migration. In contrast to the latter study, we explicitly titrated the adhesive ligation. This enabled the unambiguous demonstration that E-cadherin adhesion impedes migration and that this mechanism can predominate under certain conditions.

This adhesion-dependent reduction in cell motility could be due to strong cell attachment, which also accounts for the reduced fibroblast motility at high fibronectin densities.<sup>31</sup> It could also arise from ligation-stimulated intracellular signaling that impinges on the motility machinery by an as yet undetermined mechanism. Determining the underlying mechanism is beyond the scope of this work. However, recent studies with microdomains of fibronectin in an E-cadherin background showed that focal adhesion formation on the fibronectin correlates with the reduction in the number of cadherin adhesions on the cadherin domains under the same cell.<sup>50</sup> The competing effects of cadherin and integrins in this study may similarly reflect biochemical cross-talk that affects the organization and stability of either focal or cadherin adhesions. Future studies in this direction should begin to reveal how these two receptors mutually regulate cell motility.

Studies with mixed substrata further illustrate this coordinate control of cell motility by integrin-dependent and E-cadherin-dependent adhesion. Although E-cadherin expression and ligation impede integrin-mediated cell motility (cf. Figure 5), Figure 6 shows that increasing the fibronectin density and hence increasing integrin ligation can somewhat offset the influence of E-cadherin.

It is important to note that there are differences in the absolute migration velocities measured on mixed substrata at similar protein coverages (cf. Figures 5 and 6). On E-cadherin–fibronectin substrata, 231-Tet cells migrate faster on substrata in which fibronectin was immobilized first and then backfilled with E-cadherin (Figure 6). Conversely, when E-cadherin was immobilized first (Figure 5), the velocity was lower even though the overall protein densities were the same, within experimental error. We attribute this quantitative difference to the order in which proteins were covalently attached to the surface and to nonspecific interactions between the two proteins during patterning. Both the immobilization chemistry and nonspecific adsorption of the second protein onto the first protein immobilized could impact the activity and accessibility of both immobilized species. It is currently not possible to prevent all nonspecific cross-adsorption. Despite this, the conclusions of this study are supported by quantitative trends in data obtained with mixed protein substrata prepared by the same method (order of protein deposition). Furthermore, the qualitative trends between data sets are similarly consistent.

(49) Onder, T. T.; Gupta, P. B.; Mani, S. A.; Yang, J.; Lander, E. S.; Weinberg, R. A. *Cancer Res.* **2008**, *68*(10), 3645–3654.

(50) Tsai, J.; Kam, L. *Biophys. J.* **2009**, *96*(6), L39–L41.

The densities of E-cadherin and fibronectin that elicit these cell responses likely differ quantitatively from the physiological environment. The quantitative control of the absolute amounts of immobilized proteins was essential for demonstrating the interplay between different mechanisms regulating epithelial cell migration. However, protein adsorption and covalent attachment will impact the specific activity (activity/mg protein) of immobilized species. Nevertheless, the qualitative trends are expected to be the same, even though the absolute protein densities *in vivo* might differ, if they were quantified.

In summary, fabricated protein patterns with defined composition enabled the quantitative demonstration that E-cadherin

regulates cell motility by both adhesion-dependent and adhesion-independent mechanisms. Importantly, E-cadherin expression alone was sufficient to eliminate the dependence of the cell migration velocity on fibronectin substrata. These results further show that the predominant mechanism underlying the E-cadherin-dependent reduction in epithelial cell motility depends both on the E-cadherin expression level and on the E-cadherin density on the migratory substratum.

**Acknowledgment.** This work was supported by the National Institutes of Health grants F31 CA 126500 (to J.S.) and NIH 1 R21 HD059002 (to D.E.L.).